Academic Journal of Science and Technology
ISSN: 2771-3032 | Vol. 18, No. 3, 2025

Numerical Analysis and Research on Compressive Strength of Steel-Like Basalt Hybrid Fiber All-Light Concrete Based on Python

Wenman Jiang, Yuze Tian *, Chunliang Dong, Huaiqing Yang, Rui Hu

College of Civil Engineering, University of Science and Technology Liaoning, Anshan, Liaoning 114000, China
*** Corresponding author:** Yuze Tian

Abstract: Based on Python, this paper develops a three-dimensional mesoscopic numerical model of steel-basalt hybrid fiber lightweight concrete, aiming at revealing its compressive failure mechanism under static load. The fiber distribution model is simplified by Monte Carlo random sampling theory, and a heterogeneous composite model including aggregate, mortar, fiber and interface transition zone is established by combining the lightweight characteristics of coal gangue ceramsite as coarse aggregate. The test results show that the mixed use of basalt fiber and imitation steel fiber significantly improves the compressive strength of concrete, and the compressive strength reaches 30 MPa. The error between the simulation results and the test data is less than 3%. Comparing the mechanical properties of steel slag replacing ceramsite, it is found that the compressive strength of steel slag system is increased to 35 MPa, but the brittleness is enhanced, and the failure mode is changed from X-shaped micro-crack network of ceramsite system to concentrated splitting main crack. This study provides an efficient modeling method for micromechanical analysis of hybrid fiber lightweight aggregate concrete, and verifies the feasibility of recycling industrial solid waste.

Keywords: Imitation Steel Fiber; Basalt Fiber; All-light Concrete; Mesoscopic Simulation; Compressive Strength.

1. Introduction

With its excellent performance, concrete has become an indispensable basic material in the construction industry and is widely used in buildings, roads, bridges and marine engineering. Lightweight aggregate concrete has light weight, and its apparent density is 25%~30% lower than that of ordinary concrete. According to different application requirements and performance characteristics, it can be divided into three types: structural lightweight aggregate concrete for structural members [1]; Structural thermal insulation lightweight aggregate concrete with both structural strength and thermal insulation effect [2]; Thermal insulation lightweight aggregate concrete with emphasis on thermal insulation performance [3]. Among them, structural lightweight aggregate concrete not only has high strength and light weight, but also has good thermal insulation, crack resistance and seismic durability. These advantages make it have unique advantages in complex projects such as high-rise buildings and long-span bridges, which can improve the energy efficiency of buildings and prolong their service life. Its aggregate sources are extensive, including industrial waste residue, coal gangue abandoned by coal mines, and fly ash generated by thermal power generation, which effectively reduces the occupation of farmland and environmental pollution.

Many scholars at home and abroad have studied the mechanical properties of lightweight aggregate concrete. Huicun et al. [4] found that the mixing of basalt fiber and PVA fiber can significantly improve the flexural strength of concrete, and analyzed the optimization effect of fiber distribution on the interface transition zone. Wu Canwei et al. [5] compared the mixed impact properties of basalt fiber with carbon fiber and glass fiber, and pointed out that basalt fiber has higher surface roughness, which is more closely combined with resin matrix and shows better energy absorption ability under impact load. Guo Yinchuan et al. [6] found that the attenuation rate of bending toughness coefficient of basalt fiber reinforced concrete decreased under fatigue load, which was mainly due to the "secondary reinforcement" of fibers. At present, the research on lightweight aggregate concrete mainly focuses on macro-mechanical properties, and the numerical analysis software is less used for micro-analysis. On the meso-scale, fiber reinforced concrete is a complex multiphase material composed of aggregate, mortar, fiber and interface transition zone. The performance of fiber reinforced concrete can be simulated and predicted efficiently and accurately with the help of meso-model. Its static and dynamic mechanical properties cover material parameters [7-9], mechanical properties [10-11] and damage and fracture phenomena [12-13].

In order to study the compressive failure mechanism of steel-basalt hybrid fiber full-light concrete, a simplified method of steel-basalt hybrid fiber model based on Monte Carlo random sampling theory is proposed, and a meso-numerical model of all-light concrete is constructed through Python secondary development. Combined with the mechanical properties test, the reliability of the model is verified, and the mechanism of bridging crack resistance of fiber in concrete damage evolution is revealed. This modeling method provides a new paradigm for numerical simulation of meso-scale heterogeneous fiber reinforced concrete, and the Python analysis module developed can realize the visual representation of the whole meso-damage process of lightweight aggregate concrete. The purpose of this study is to provide theoretical support for the optimal design of hybrid fiber concrete and the application of solid waste resource.

2. Test and Mix Proportion

2.1. Raw Materials

In this study, P O32.5 ordinary portland cement and class I fly ash are used as cementing materials, the coarse aggregate is coal gangue ceramsite with a particle size of 5~10mm (bulk density is 844 kg/m, barrel compressive strength is 6.2MPa, silt content is less than 0.1%, and water absorption rate is 8.4%), and the fine aggregate is natural river sand with fineness modulus of 2.7. The benchmark mixture ratio is: cement 370 kg/m, fly ash 160 kg/m, coal gangue ceramsite 475 kg/m, natural river sand 760 kg/m, water 215 kg/m, and polycarboxylic superplasticizer 5.3 kg/m is added. Basalt fiber (30mm in length, 7-15 μ m in monofilament diameter, 2.65 g/cm in density, 100GPa in elastic modulus and 4200MPa in tensile strength) and imitation steel fiber (45mm in length, 5-18μm in monofilament diameter, 0.98 g/cm in density, 7.6GPa in elastic modulus and 500MPa in tensile strength) are selected as fiber materials for hybrid reinforcement. Basalt fiber, imitation steel fiber and coal gangue ceramsite used in the experiment are shown in Figure 1~ Figure 3 respectively.



Fig 1. Basalt fiber

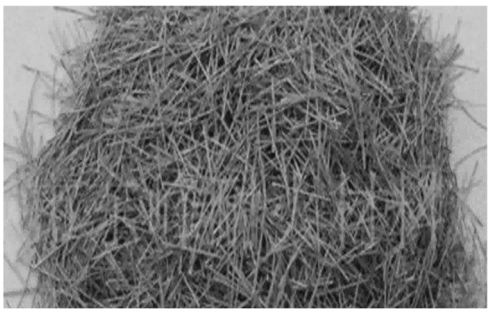


Fig 2. Imitation steel fiber

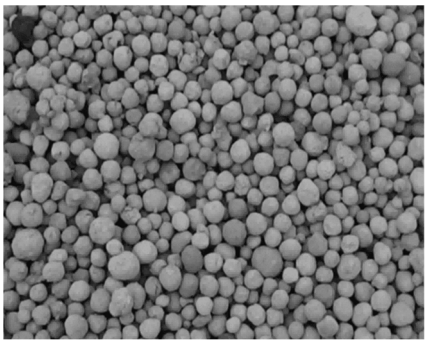


Fig 3. Coal gangue ceramsite

2.2. Mixture Ratio

The benchmark concrete mixture ratio of this test is designed according to Code for Design of Ordinary Concrete Mixture Ratio (JGJ55—2011). Coal gangue ceramsite is used to replace natural stones as coarse aggregate with volume fractions of 10% and 12% respectively, and imitation steel fiber and basalt fiber are mixed into concrete matrix to construct a binary fiber synergistic reinforcement system, as shown in Table 1. Three 100mm×100mm×100mm cube specimens were made in each group. Considering the water absorption property of ceramsite, the specimen is pre-wetted for 1 day before making.

Table 1. Mix Proportion of Imitation Steel-Basalt Hybrid Fiber Full Lightweight Concrete (kg m-3)

number	cement	flyash	pebble	ceramsite	fine aggregate	water	high efficiency water reducing agent	Basalt fiber	Imitation steel fiber
01	370	160	427.5	47.5	760	215	5.3	1.0	3.0
02	370	160	427.5	47.5	760	215	5.3	2.0	3.0
03	370	160	427.5	47.5	760	215	5.3	3.0	3.0
04	370	160	668.8	91.2	760	215	5.3	1.0	1.0
05	370	160	668.8	91.2	760	215	5.3	2.0	1.0
06	370	160	668.8	91.2	760	215	5.3	3.0	1.0

3. Test Results and Analysis

After curing for 28 days under natural conditions, the mechanical properties of the specimens were measured according to the Standard for Test Methods of Physical and Mechanical Properties of Concrete (GB/T50081—2019). The compression test of test blocks 01~06 is shown in Figure 4, and the compressive strength is shown in Figure 5. C30 concrete substitute products are made of 10% (47.5 kg m-3) coal gangue ceramsite, 0.05% (2.0 kg m-3) basalt fiber and 0.15% (3.0 kg m-3) imitation steel fiber, and the strength is about 30MPa.

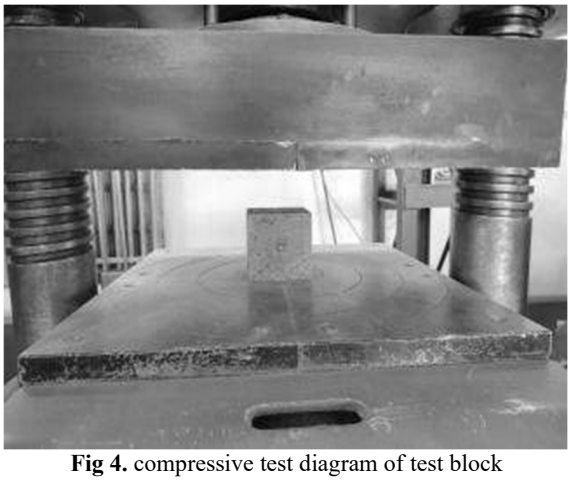


Fig 4. compressive test diagram of test block

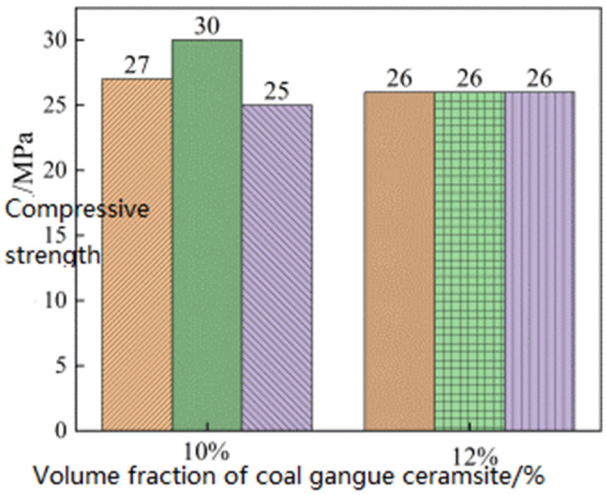


Fig 5. compressive strength of test block

4. Numerical Simulation

4.1. Model Building

The internal structure of concrete is heterogeneous and random, which leads to the complex nonlinear mechanical response of the material at the macro scale. From the microscopic point of view, this study regards basalt fiber reinforced concrete as a composite system composed of cement slurry, coarse aggregate, fiber and the interface transition zone between cement slurry and coarse aggregate [14-16]. According to the proportion determined by the experiment, the numerical simulation software is redeveloped by Python language to realize the pre-processing of the simulation model.

In the numerical analysis, the irregularly shaped stones are assumed to be dodecahedron, and the spherical coal gangue ceramsite is simplified to a sphere. Using Monte Carlo random sampling method, aggregate coordinates are randomly generated in Cartesian coordinate system.

$$\begin{cases} z = \mathrm{r}_{size} * cos(angle_1) \\ x = \mathrm{r}_{size} * sin(angle_1) * cos(angle_2) \\ y = \mathrm{r}_{size} * sin(angle_1) * sin(angle_2) \end{cases} \quad (1)$$

Where: rsize is the characteristic size of aggregate particle size, mm; θ is polar angle, rad, ranging from 0 to π; φ is azimuth, rad, and the range is 0~2π.

The two kinds of fibers are considered as beam elements in the numerical analysis software, and they are randomly distributed between 0 and 2π. It is distinguished by the material properties and length changes of its fibers. The quantity of fiber shall be put in according to the test proportion, and the fiber shall not cross the aggregate.

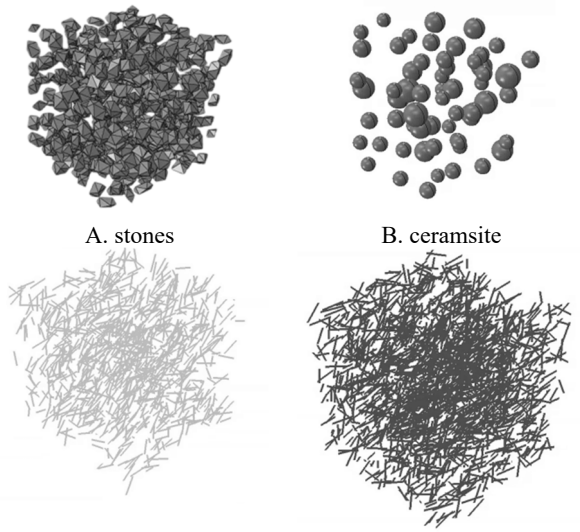


Fig 6. Model diagram of cubic specimen

4.2. Material Properties

The material property value of coarse aggregate comes from its own rock mass property, and its elastic modulus is about 60GPa according to literature [17]. Because the coarse aggregate and fiber are not damaged when the specimen is damaged, two kinds of coarse aggregate and two kinds of fiber are considered as linear elastic bodies in numerical simulation, and the material parameters of each component are shown in Table 2.

Table 2. Material parameters of concrete components

Meso-composition of concrete	Elastic modulus /GPa	Compressive strength /MPa	Tensile strength /MPa
pebble	56.0	55.0	200.0
ceramsite	3.0	25.0	20.0
Basalt fiber	100.0	—	4200.0
Imitation steel fiber	7.6	—	500.0

4.3. Contact Setting

Through finite element modeling and analysis, C3D8R solid elements are selected for the upper end plate, aggregate, mortar and interface transition zone. The end plate is set as a rigid body; The fiber adopts B31 unit. In the model, the top plate is in contact with mortar, and the contact properties are defined by "normal behavior" and "tangential behavior" in surface contact. In tangential direction, the friction coefficient is set to 0.6. In the steel-concrete interface, the normal contact relationship follows the "hard contact" rule, the fiber is implanted into the concrete matrix through the "embedded area method", the concrete bottom adopts fixed contact, and the axial force is applied to the upper end plate through displacement loading, as shown in Figure 7. The coefficient of friction is set to 0.6. In the steel-concrete interface, the normal contact relation follows the rule of "hard contact"

4.4. Comparison between Finite Element Results and Experiments

After the 28d curing period, the cube compressive test was carried out according to the Standard for Test Methods of Physical and Mechanical Properties of Concrete (GB/T50081—2019). The test data and numerical simulation results are shown in Figure 8~ Figure 9.

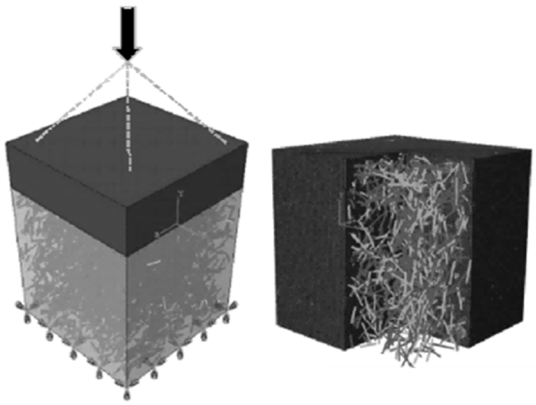
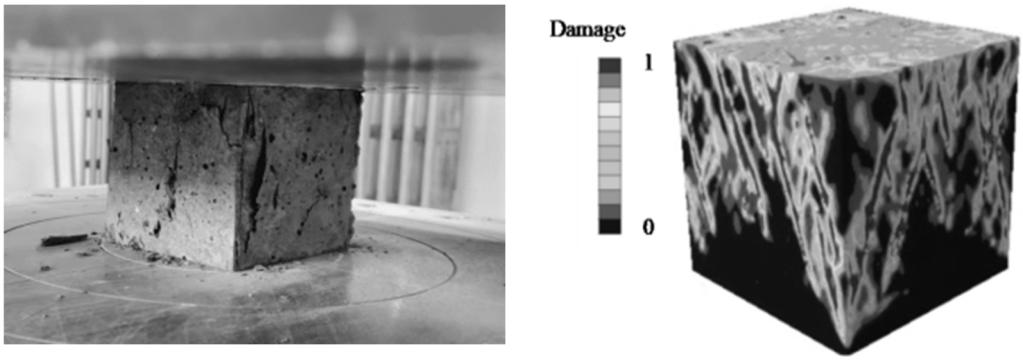


Fig 7. schematic diagram of cubic specimen loading

Because the performance of concrete is influenced by material characteristics, test equipment and curing conditions, it is easy to lead to the deviation between the test results of mechanical properties and the numerical simulation results. The mechanical properties of fiber reinforced concrete are predicted and analyzed by referring to the experimental data of ordinary concrete and adjusting the parameters of each component in the model. The results show that the failure mode of the simulated block is similar to the experimental failure mode, and the error between the numerical simulation results and the experimental data is strictly controlled within 3%. This shows that the compressive numerical model of steel-like basalt hybrid fiber lightweight concrete based on Python can accurately reflect the mechanical strength characteristics of concrete under static load.



A. Failure diagram of test block B. Simulated damage diagram

Fig 8. Comparison of failure modes of test blocks

4.5. Failure Mechanism Analysis

In the cube compressive test, micro-cracks gradually spread and formed staggered cracks, which eventually led to the failure of the specimen. The cracks are mainly concentrated in the central area of concrete, while the parts near the loading plate are relatively intact. The damage degree in the middle part of the specimen is obviously greater than that in the end part of the loading plate, and the damage phenomenon in the middle part of the axial compression specimen is more obvious.

The meso-simulated failure process of cubic compressive test is shown in Figure 10. At the initial stage of loading, the interface layer around the concrete aggregate first appeared damage. With the continuous increase of pressure, some aggregate interface layers began to form cracks, and the corner areas also showed signs of damage. Because the strength of aggregate is significantly higher than that of mortar, cracks will extend to the weak parts that are easier to expand, thus minimizing energy dissipation. When the damage area of the interface layer reaches a certain threshold, damage marks appear at the corners. Because the strength of aggregate far exceeds that of mortar, cracks will spread to weaker parts to reduce energy consumption. When the damaged area of the interface layer expands to a certain extent, the crack will bypass the aggregate and connect with the adjacent damaged interface layer, forming a penetrating main crack, and finally forming an X-shaped profile with an angle of 45 on the outer surface. The uniform distribution of aggregate and fiber makes the overall strain of concrete more uniform, forming a complex and wide crack path, and the damage profile of the outer surface is X-shaped and gradually shrinks to the core. In contrast, the two inverted cone areas near the loading plate have less damage and show obvious "hoop effect". There are signs of damage. Because the aggregate is much stronger than mortar, cracks can propagate to weaker areas to reduce energy consumption. When the damage area of the interface layer is enlarged to a certain extent, the crack will bypass the aggregate and connect with the adjacent damage interface layer, forming a penetrating main crack, and finally forming an x shape contour with 45° angle on the outer surface. The uniform distribution of aggregate and fiber makes the overall strain of concrete more uniform and forms a complex and wide crack path. The damage profile on the outer surface is x shape and gradually shrinks to the core. In contrast, the two inverted cone regions adjacent to the loading plate exhibited less damage and exhibited a significant "hoop effect".

At the initial stage of loading, the mortar matrix of cubic specimens is the main load-bearing structure, and the fibers are idle. With the loading of the specimen, the mortar matrix and fiber move relatively, and the interaction between them is mainly chemical bonding force, which inhibits the development of interfacial shear stress. When the load continues to increase, the number of fibers participating in the stress gradually increases until the cracks in the internal interface layer of concrete penetrate each other, forming an X-shaped profile with wide ends and contraction in the middle. This phenomenon can be attributed to the lateral displacement caused by Poisson effect when concrete is compressed: the deformation near the loading plate is small due to the end restraint, and the lateral deformation in the middle area is significant, resulting in the X-shaped distribution of the damaged area. In addition, the deformation

of the matrix intensifies the debonding between the fiber and the matrix, which makes the fiber stress in the damaged area increase gradually with the damage extension.

There is a significant difference in stress response between imitation steel fiber and basalt fiber during this process. Because of the low elastic modulus, weak tensile strength and poor bonding performance with the matrix, imitation steel fiber is more likely to debond and slip when the matrix damage is aggravated, which leads to stress redistribution through friction and stress relaxation. Basalt fiber, with its high elastic modulus, high strength and strong interfacial chemical bonding, can effectively transfer load, inhibit crack propagation and maintain a stable stress state. Imitation steel fiber is long and sparsely distributed, and the slip increases after debonding, which further aggravates the stress attenuation; Basalt fibers form a three-dimensional reinforced network because of the dense distribution of short fibers, which delays the damage accumulation. In addition, the transverse deformation caused by Poisson effect makes the low-modulus imitation steel fiber bear multi-directional stress, which disperses its bearing capacity. Basalt fiber resists deformation through high stiffness and dominates the axial stress transmission. In the end, there is a significant difference in mechanical behavior between them during the failure process.

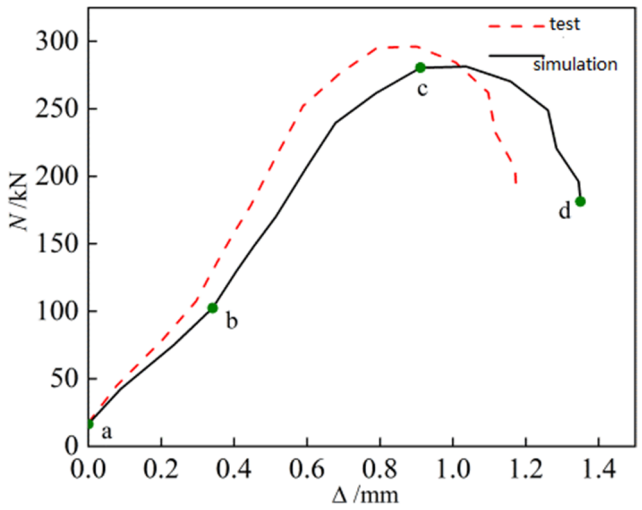


Fig 9. Comparison of load-displacement curves of test blocks

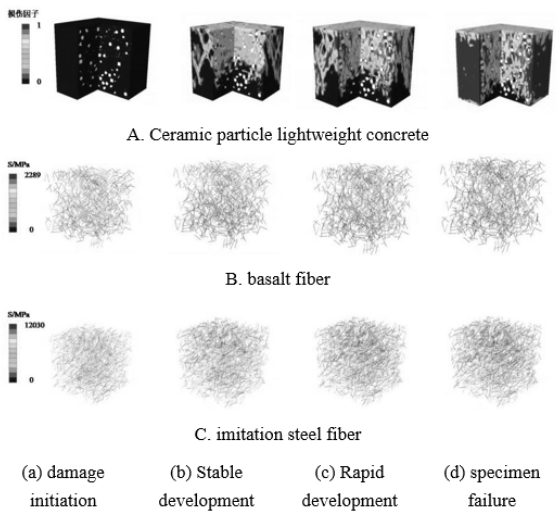


Fig 10. Failure process diagram of steel-basalt hybrid fiber all-light concrete

4.6. Parametric Analysis

As a kind of solid waste produced in steelmaking process, steel slag's high hardness and density can significantly improve the compressive strength of concrete. The elastic modulus is about 5 GPa, Poisson's ratio is about 0.25, the density is 11 500 kg/m, and the predicted compressive strength can reach 35 MPa, which is higher than 30.1 MPa of ceramsite system. Although the porous structure of ceramsite reduces the rigidity of concrete, the bonding performance between fiber and matrix is better, and the failure process shows better ductility. Fig. 11 shows the load-displacement curves of ceramic lightweight concrete and steel slag concrete. Cracks in steel slag system tend to propagate along the steel slag-mortar interface, forming a few wide main cracks, and the failure is characterized by brittle splitting. Fiber bridging is limited by interface slip, and the final failure surface is relatively flat. The cracks in ceramsite system bifurcate and expand along the ceramsite pores and interface transition zone, forming a dense micro-crack network. Basalt fibers restrain the crack width through three-dimensional reinforcement, and the failure surface is rough and presents an X-shaped profile. The comprehensive utilization of steel slag can not only effectively reduce the waste of resources and environmental pollution, but also provide high-performance alternative raw materials for building materials such as concrete, which has remarkable economic and environmental benefits.Density can significantly improve the compressive strength of concrete. Modulus of elasticity approx. 5 GPa, Poisson's ratio is about 0.25 and the density is 11500 kg/m³

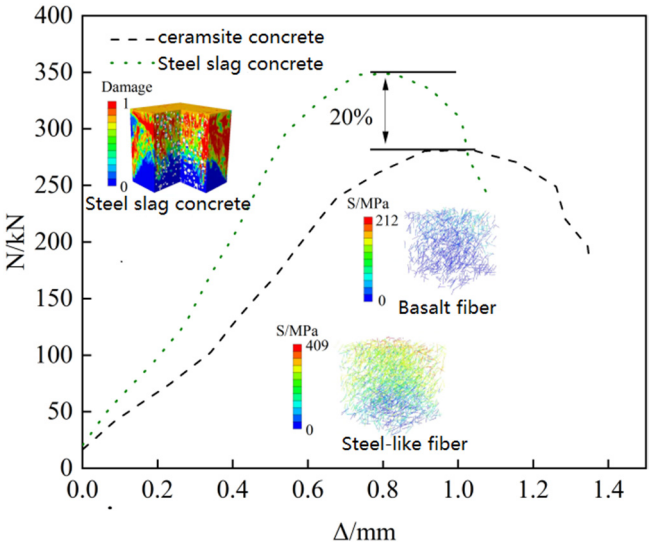


Fig 11. Load-displacement curves of ceramic lightweight concrete and steel slag concrete.Load-displacement curves of ceramsite all-light concrete and steel slag concrete

5. Conclusion

1. Python-based three-dimensional mesoscopic model can accurately predict the compressive strength of steel-like basalt hybrid fiber lightweight concrete, and the error between simulation results and experimental data is less than 3%, which verifies the applicability of Monte Carlo random sampling method in fiber distribution modeling.

2. Basalt fiber leads the load transfer through high modulus and strong interface bonding, and imitation steel fiber leads to stress relaxation due to debonding and sliding. The cooperation of the two can significantly improve the compressive strength of ceramsite concrete, reaching 30MPa.

3. After replacing 10% stones with steel slag, the compressive strength is increased to 35 MPa, and the interface bonding is weak, which leads to brittle failure; Coal gangue ceramsite system shows X-shaped micro-crack network due to uniform pore distribution, and its ductility is better.

Take part in the examination and contribute.

Acknowledgments

Fund Project: University Students Innovation and Entrepreneurship Project of Liaoning University of Science and Technology, Project No.: X202510146384.

References

[1] Zhang Zhipeng, Zhang Kaizhang, Wu Fei. Study on dynamic compressive properties of carbon fiber lightweight aggregate concrete after high temperature [J]. Concrete, 2024(4): 67-70, 127.

[2] Song Tao, Su Xiangdong, Wang Shuaihui, et al. Study on the influence of expanded perlite on the performance of one-component lightweight aggregate concrete [J]. Brick and tile, 2024(12): 54-57.

[3] Yan Xiangyang, Xia Huiyun. Study on the influence of the content of polystyrene particles on the mechanical properties and thermal insulation properties of concrete [J]. Functional Materials, 2024, 55(9): 9214-9221.

[4] Hui Cun, Cao Xu, Liu Pan, et al. Study on mechanical properties of basalt -PVA hybrid fiber concrete [J]. Journal of Zhongyuan University of Technology, 2018, 29(6): 32-36.

[5] Wu Canwei, Zhang Zuoguang, Sun Zhijie, et al. Study on the impact properties of basalt fiber hybrid composites [C]// Proceedings of the 5th inaugural meeting of composite professional committee of China Aviation Society and the symposium on new technologies and applications of aviation composite materials. Beijing: China Aviation Society, 2005:175-181.

[6] Guo Yinchuan, Liu Hongchang, Shen Aiqin, et al. Toughness characteristics and attenuation law of basalt fiber bridge concrete [J]. Journal of Chang 'an University (Natural Science Edition), 2023, 43(2): 89-99.

[7] LIANG X W, WU C Q. Meso-scale modelling of steel fibre reinforced concrete with high strength[J]. Construction and Building Materials, 2018, 165: 187-198.

[8] SU Y, LI J, WU C Q, et al. Mesoscale study of steel fibre-reinforced ultra-high performance concrete under static and dynamic loads[J]. Materials & Design, 2017, 116: 340-351.

[9] Jin Liu, Du Xiuli. Dynamic failure behavior analysis of concrete based on meso-element equivalence method [J]. Engineering Mechanics, 2015, 32(4): 33-40.

[10] Xie Pengtao, Wu Chengqing, Liu Zhongxian, et al. Numerical simulation of SHPB test of ultra-high performance steel fiber reinforced concrete based on meso-model [J]. China Science: Physics and Mechanics Astronomy, 2020, 50(2): 131-143.

[11] CHEN Q, ZHU H H, YAN Z G, et al. A multiphase micromechanical model for hybrid fiber reinforced concrete considering the aggregate and ITZ effects[J]. Construction and Building Materials, 2016, 114: 839-850.

[12] Xiong Wang, Qin Shuhao, Peng Dingdong, et al. Numerical simulation of basalt fiber reinforced concrete based on three-dimensional mesoscopic model [J]. Journal of Building Science and Engineering, 2024, 41(1): 181-190.

[13] Jaco. Analysis of tensile fracture behavior of meso-concrete based on cohesion model [J]. Journal of Jiangsu Institute of Architecture, 2024, 24(3): 9-14.

[14] Jin Liu, Wang Zhongshiyu, Zhu Huajie, et al. Meso-numerical analysis of the size effect of concrete-filled steel tubular columns under pure torsion [J]. journal of basic science and engineering, 2023, 31(3): 780-793.

[15] Jin Liu, Jia Likun, Zhang Renbo. Meso-numerical study on fracture behavior of steel fiber reinforced concrete at low temperature [J]. Engineering Mechanics, 2023, 40(S1): 200-206.

[16] Jin Liu, Zhu Huajie, Du Xiuli. Numerical analysis of the size effect of reinforced concrete columns under pure torsion [J]. Engineering Mechanics, 2022, 39(7): 227-236.

[17] Jin Liu, Li Jian, Yu Wenxuan, et al. Meso-numerical simulation study on dynamic biaxial tension-compression failure criterion of concrete [J]. Journal of Mechanics, 2022, 54(3): 800-809.